THE MISFIRE DEGREE AND ITS EFFECTS ON COMBUSTION AND POLLUTANT FORMATION OF SUBSEQUENT CYCLES
A Study on a High Speed Gasoline Engine

by

Yangyang CHEN[a], Qifei JIAN[a], Banglin DENG[b*], and Kaihong HOU[b]

[a] School of Mechanical and Automotive Engineering,
South China University of Technology, Guangzhou, Guangdong, China
[b] College of Mechatronics and Control Engineering,
Shenzhen University, Shenzhen, China

https://doi.org/10.2298/TSCI210606292C

Misfire has attracted lots of researcher's attention as a common engine fault, but most researchers focus on misfire diagnosis. For motorcycle engines, misfire is more worth to investigate because of the more extensive operation windows. The misfire degree is detected by experiment and its effect mechanism on subsequent cycles is investigated through simulation. Its effect is analyzed through two aspects. First, misfire cycle leaves about 10.8% fuels that participate in next cycle working process, leading to richer fuel/air mixture. But 13.8% lower of in-cylinder peak pressure than normal scenario is observed. Then interaction between flame propagation and flow field is discussed. The effect of misfire on flow field intensity is small, but it changes flow field structure largely. This change evolves persistently during subsequent processes, superimposing the lower temperature brought by misfire of last cycle, resulting in slower flame propagation and thus lower thermal efficiency for misfire scenario. This impact can last 3-4 subsequent cycles until gradually fades away. Second, for pollutants formations, the NO emission is lower for misfire scenario due to the lower in-cylinder temperature, but HC emission is higher. Although higher CO is produced during main combustion phase for misfire scenario, it converts to CO_2 more largely during post flame stage, resulting in almost the same final amount relative to normal scenario.

Key words: *gasoline engine, misfire, energy conversion, flow field, flame propagation, CFD*

Introduction

With development of fundamental theories, new technologies, and responding the energy conservation and emission reduction, more and more cleaner energies are developed and applied for driving a car in recent years, such as hydrogen, or electric energy. However, they are not applied in a large scale because of the limitation of some key technologies (for example cruising ability, operation stability). Internal combustion engines (ICE) are still the main power machinery used in automobile industry. According to China Mobile Source Environment Management Annual Report [1], the number of automobiles reaches 260 million until 2020 in China, among them the proportion of powered by fossil fuel and new energy are 98.5% and 1.5% (3.81 million), respectively. Thus, it is very necessary to investigate the fac-

* Corresponding author, e-mail: dengbanglin123@126.com

tors, which cause bad engine performances (such as high fuel consumption and emission), and optimize them.

For premixed combustion engine, the engine performance mainly depends on the in--cylinder combustion process. In previous investigations [2, 3], it has been summarized that the in-cylinder combustion process is mainly affected by following three factors in gasoline engine: the effect of engine structure (such as compression ratio, location and number of spark plugs), the effect of quality and component of air/fuel mixture, and the effect of operation conditions (engine speed, load). Among them, engine structure affects flame propagation by generating different flow patterns. Deng *et al.* [4] analyzed the interaction between flame propagation and flow field in three different engine structures in detail, the result showed that during flame propagation the smaller distance between flame center and flow field center could generate better combustion performance (for example smaller combustion variation between cycles). Chen *et al.* [5] utilized the twin-spark ignition model to shorten combustion period (twin-spark ignition model generated higher turbulence kinetic energy (TKE) to accelerate the flame propagation) and then acquire the higher torque and lower fuel consumption. The effect mechanism of air/fuel mixture on engine performance is different from engine structure, it impacts on engine performance by influencing combustion efficiency and flame propagation speed. Deng *et al.* [6] found that when the excess air coefficient, λ, increased from 0.85-1.2, the engine torque decreased by 20.3% under 60% load and 3000 rpm, the decrease was even more significant at other operating conditions. A similar phenomenon was found by Ossama *et al.* [7], they found that the fastest laminar flame speed was generated under $\lambda = 0.9$ for iso-octane, and only when the width of λ was kept at a range of 0.8 to 1.2, the combustion process is normal. Otherwise, flame propagation will be difficult during combustion stage, even occurs the misfire phenomenon, especially for motorcycle engine because of the more extensive operation conditions. Thus, if the engine performances want to be improved further, it is well worth to research the effect mechanism of misfire on in-cylinder work process of subsequent cycles.

Misfire is a common fault for ICE. Abhishek *et al.* [8] and Jafarmadar *et al.* [9] have summarized some factors, which cause the misfire phenomenon, and they also stated that misfire reduced engine power output by 25% and increased fuel consumption and emissions. Thus, misfire behavior of engine attracts a lot of researchers to find some high-efficiency methods to accurately detect misfire. For example, Masayuki *et al.* [10] combined the exhaust temperature with an algorithm to detect misfire, this method could attain 75% successful detection ratio. Andrew *et al.* [11] used a combination of digital filtering (residual generation) and statistical pattern recognition (fault isolation) to detect the intermittent and continuous misfire through separate algorithms, the intermittent misfire phenomenon could be detected 100% for all conditions, continuous misfire was also detected accurately when the engine speed is below 4000 rpm. In the past few years, lots of experiments or novel methods focused on the misfire detection [12-14]. However, the research about effect mechanism of misfire is very rare during subsequent work process, especially for small displacement gasoline engine.

In order to figure out the aforementioned problem and further understand the misfire effects, the research method of experiment combined with numerical simulation was used in this study. A single-cylinder engine used for motorcycle was tested, the misfire degree under both steady-state and transient operations were evaluated, then a 3-D in-cylinder model was built and calculated by a commercial CFD software based on the real experiment condition. The goal of this study is to explore the misfire degree and its effect on flow field structure and combustion process in subsequent cycles. We hope to provide an implication for developing higher performance engines especially decreasing fuel consumption and emission.

Experiment set-up

The experiment was performed on a single-cylinder, four-stroke motorcycle engine. Its displacement is 125 mL, the detailed engine parameters are displayed in tab. 1. The equipment used in experiment and their parameters are listed in tab. 2. Figure 1 shows the diagram of experimental set-up and the distribution of sensors, there are two test scenarios in the current study: steady-state and transient detection, respectively. The steady-state experiment process has been described in detail in previous research [5], only a brief description is given in following.

Table 1. Engine parameters

Item	Content	Item	Content
Engine type	Four-stroke and single-cylinder, single-spark	Connecting rod length [mm]	103.5
Displacement	125 mL	Compression ratio	9.0
Bore [mm]	56.5	Maximum power [kW]	8.3
Stroke [mm]	49.5	Maximum torque [Nm]	10

Table 2. Test equipments

Equipment name	Manufacturer/type	Measurement range	Precision
Dynamometer	API-COM/100 kW 9157-08-3	0-100 kW	1 Nm
Emission tester	AVL/Digas2200	CO: 0-10%vol NO: 0-5000 ppm	CO: 0.01%.vol HC: ±1 ppm
Combustion analyzer	DEWESOFT/SIRIUSi-HS CA	0-200 V	200 ks/s
Fuel consumption meter	API-COM/MC 082	0-50 kg/h	±0.10%
Cylinder pressure sensor	Kistler/6115BFD34Q02	0-100 bar	–9.692 bar/v
Intake pressure sensor	Kulite/XTL-190M-500 kPa	0-5 bar	0.199 mV/kPa
Exhaust pressure sensor	Kulite/EWCTV-312M-17BARA	0-10 bar	265.691 mV/bar

During steady-state experiment, in order to ensure the experimental data is reliable enough, the data were collected under engine operation more than 300 cycles. The engine operated under a wide range of condition. For example, the engine load was 30%, 60%, and 100%, respectively, the operation range of speed was within 3000 rpm to 9500 rpm, and the interval was set to 500 rpm. Under all conditions, the excess air coefficient, λ, is 1. In each case, some important engine operating parameters, such as intake, exhaust pressure, were measured and collected. The performance parameters, such as torque and brake specific energy consumption and so on, were also measured and collected. The in-cylinder pressure was measured by a special pressure sensor (Kistler/6115BFD34Q02) to reflect the in-cylinder combustion situation (the misfire degree), the sampled interval was set to 0.1 °CA. The heat release rate (HRR) generated by fuel was measured by a combustion analyzer (DEWESOFT/SIRIUSi-HS CA) also with an interval of 0.1 °CA. During the test, all of data

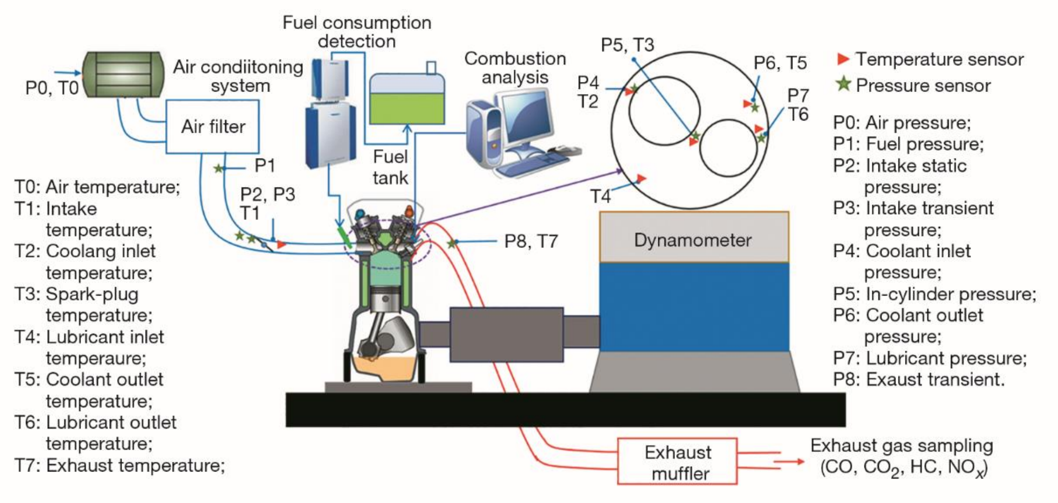

Figure 1. Schematic diagram of experiment set-up

were acquired when the engine was preheated fully, the criterion is that temperature of spark plug reached 120° ±5° with a 30 seconds stable operation. The environment temperature and pressure, for both steady-state and transient experiments, were controlled at 25° ±1° and 1 bar ±100 Pa.

For transient detection, the combustion process is reflected by vibration signal. An accelerometer was used to measure the vibration on the surface of engine cylinder head. During this test, after warming, the engine was initially operated at low speed (~3000 rpm) and medium load for about 15 seconds, then the speed was suddenly raised up to highest ~9000 rpm while the engine load was declined, so that it may happen misfire. A well calibrated algorithm is used to estimate misfire. This algorithm uses a relative vibration signal (a measured value divided by a reference value that measured under misfire scenario) that involves engine operation parameters (speed/load) as a misfire indicator.

The CFD set-up and verification

In this study, the simulation was performed by a commercial software named CONVERGE [15], it is more efficient and professional for calculating the in-cylinder work process relative to other software. The RNG k-ε model is selected to simulate the development of in-cylinder turbulence [16]. A reduced skeletal chemical model was used to emulate the in-cylinder combustion process [17]. In this model two components, iso-C8H18 (90 vol.%) and n-C_7H_{16} (10 vol.%), were used to represent the realistic gasoline. To trade off the calculation precision and cost, the process of grid arrangement strategy is introduced: first, according to our multiple tries and the grid-independence study of Rakopoulos *et al.* [18], the base grid size of 8 mm was selected; second, the refinement level of 2 (half grid size relative to base grid) was applied to cylinder and for capturing the discharge process, at spark plug location two layers refinement levels of 2, 4 are arranged, respectively; third, in order to capture the drastic change of temperature and velocity, adaptive mesh refinement was used with 3 refinement levels during flame propagation (–32 to 80 °CA). After aforementioned grid refinement scheme, the minimum grid size of 0.25 mm can be attained, this grid strategy is enough to capture the combustion process [19].

In order to investigate the effect of misfire on engine performance, especially for flame propagation of subsequent cycles, five consecutive cycles of two scenarios were set for calculation. In Scenario 1, it is a normal working status, all boundary conditions were acquired from the experiment, and this case gives a base reference. In Scenario 2, the ignition source of second cycle was removed to simulate the misfire phenomenon during five consecutive cycles. The rest of settings in Scenario 2 were consistent with Scenario 1. For all cases, the operation condition is 5000 rpm, 60% engine load and $\lambda = 1$, the ignition timing is –31 °CA. The main boundary conditions are exhibited in following.

The transient intake and exhaust pressure were measured by experiment, which is shown in fig. 2(a). The 0 °CA is combustion TDC of cycle 1.

The intake and exhaust valve lifts are showed in fig. 2(b), and the movement trail of piston is automatically by CONVERGE.

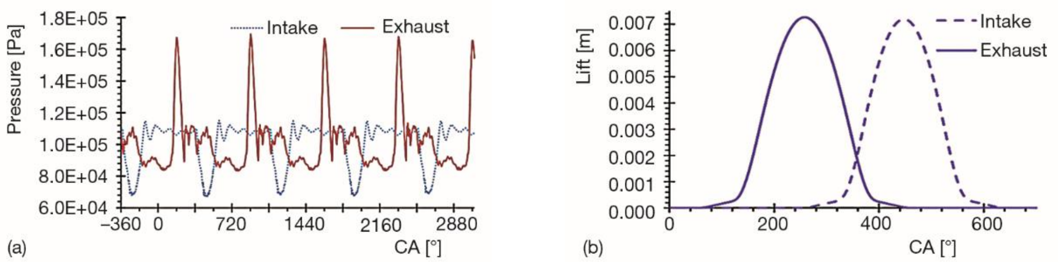

Figure 2. The measured boundary conditions; (a) the intake and exhaust pressure and (b) the valve lifts of intake and exhaust

The main wall temperatures are: intake port (425 K), chamber (450 K), cylinder wall (450 K), piston top (480 K), and exhaust port (450 K).

In order to attain the ideal convergence, the residual was set to 10^{-4} during calculation. Finally, most parameters are below it. For verifying the reliability of calculation results, the peak pressure, P_{max}, and emissions from calculation (Scenario 1) were selected to compare with experimental. Figure 3 displays the comparison of P_{max} and its location of five subsequent cycles between experiment and calculation. It can be seen that whatever the P_{max} or its location, the error between experiment and calculation is very small (the maximum error of P_{max} is 3.1%, the maximum error of location is 5.3%). Figure 4 shows the comparison of emissions between experiment and calculation. It can be found that when the NO and CO emissions from calculation are stable, it is very close to that of experiment. Thus, our calculation is enough reliable to reflect the real in-cylinder working process.

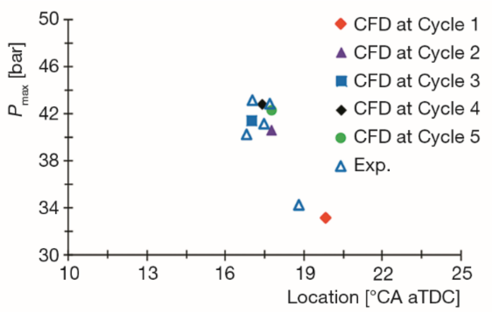

Figure 3. The comparison of P_{max} between experiment and calculation

Results and discussions

Misfire phenomenon and its degree

In general, in-cylinder combustion is divided into three levels: normal combustion, partial combustion, and complete misfire. These combustion levels can be directly detected by

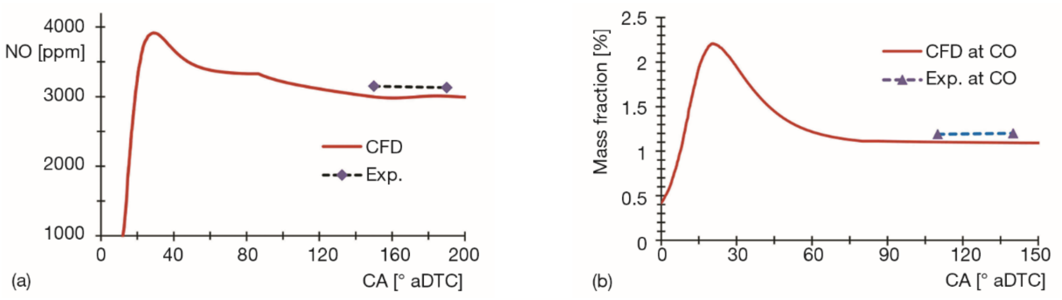

Figure 4. The comparison of emissions between experiment and calculation

detecting some important process parameters, such as in-cylinder pressure. Also, they can be indirectly reflected by collecting vibration signal and demodulating to reference value [20]. In this work, under steady-state detection, the direct method is used (namely the in-cylinder pressure measurement), while under transient operation the indirect method is used due to the response difficulty in in-cylinder measurement during high transient operation. Figure 5 displays the combustion levels of 300 cycles under a wide operation conditions. Referring to [21], the heat release percentage *vs.* indicated mean effective pressure (IMEP) is used to indicate the combustion completeness degree. It can be seen that under low engine speed the combustion process is very excellent, almost all cycles are normal combustion. But, cycles of partial combustion increase with increase of speed, especially for operation conditions of 5000 rpm, 60%, load and 9000 rpm, 30% load. Under these two conditions, the combustion process of some cycles are very poor. Though those cycles are partial combustion, they almost equal to misfire due to very little combustion heat is released. Because the in-cylinder working process is continuous, these cycles will have obvious effect on engine performance. But, due to the limitation of detection technology, it is very difficult to observe their effects by experiment. Thus, in order to further understand the effect of misfire on continuous working process, we design an extreme simulation scenario (complete misfire) to analyze what happen during this process.

According to the study of Peterson *et al.* [22], the misfire was not result of failed ignition during engine operation, but a failure of flame propagation because of the leaner mixture and lower velocity near spark plug. It means that the structure of flow field, the composition of air/fuel mixture in misfire cycle will generate significant differences from normal cycles and then affect subsequent cycles. The working process of ICE is sequential, how much the effect of misfire cycle on subsequent cycles, which need to further investigate. Figure 6 compares the in-cylinder pressure evolution of sequential five cycles between normal and misfire scenarios. It can be seen that the in-cylinder pressure of cycle 2 is obviously lower than other cycles because of the lack of ignition source in misfire scenario (see the dashed circle). From fig. 6, at least three aspects can be observed regarding the effect of misfire cycle on following cycles: Comparing normal and misfire scenarios, the in-cylinder pressure of cycle 3 (the next cycle after misfire cycle) in misfire scenario is significantly lower than normal scenario (the peak pressure of cycle 3 in misfire scenario is 36 bar, the normal scenario is 41 bar). In misfire scenario, the variation of cylinder pressure in the next few cycles after misfire cycle is obviously higher than the normal scenario; in normal scenario, the highest variation of cylinder pressure is 3.98% (between cycle 4 and cycle 5), but in misfire scenario the highest variation reaches to 11.92% (between cycle 3 and cycle 5, note that this value is only

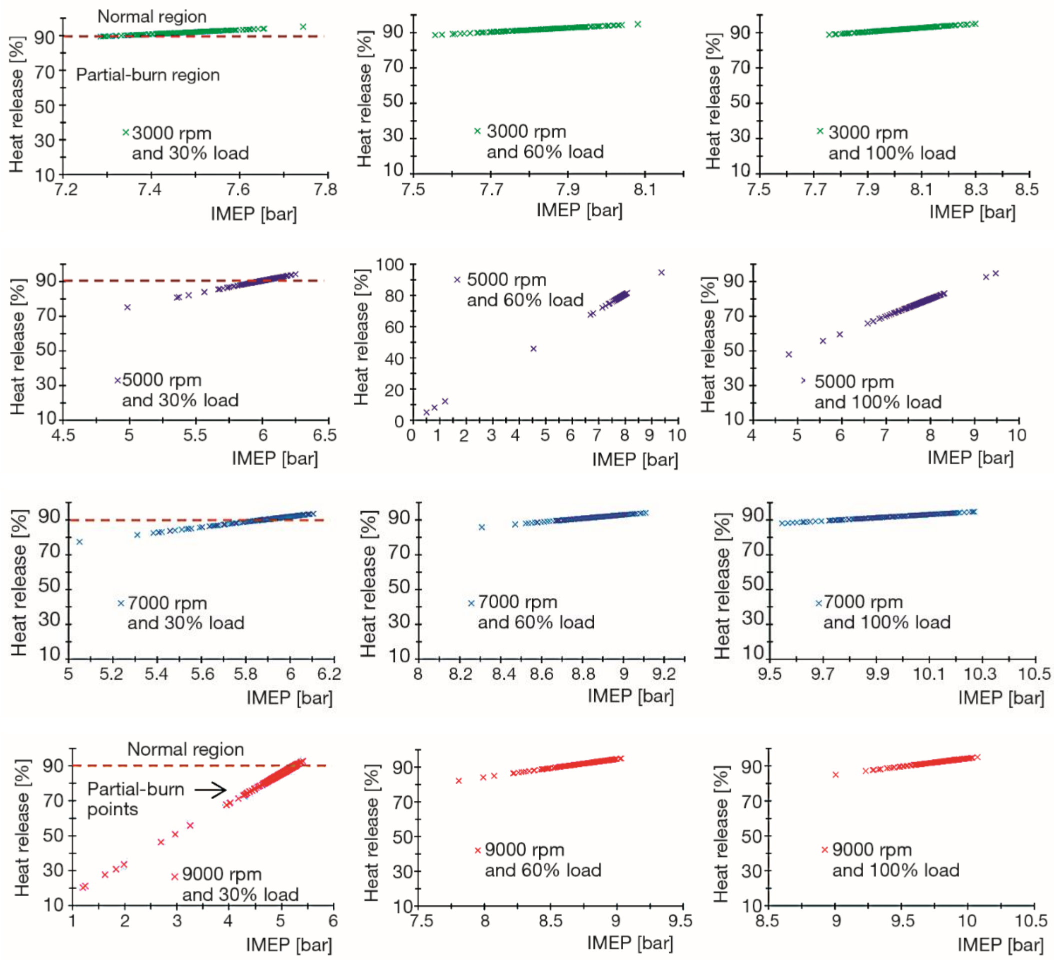

Figure 5. The heat release percentage *vs.* IMEP for 300 consecutive cycles

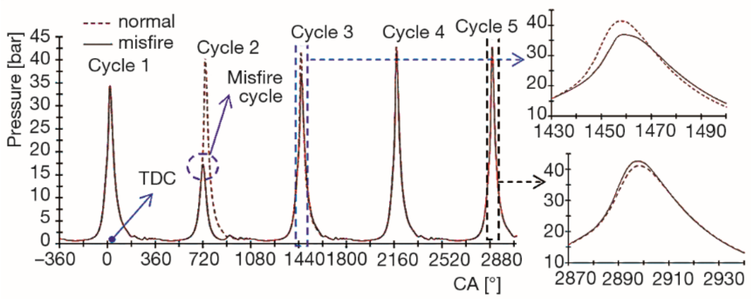

Figure 6. The evolution of cylinder pressure with CA evolved for sequential five cycles

0.97% in normal scenario); this phenomenon will contribute to higher cycle-to-cycle variation. The effect of misfire cycle on subsequent cycles is persistent, at least the effect still exists in cycle 5; after which, however, its impact gradually reduces; for example, whatever the evolution of cylinder pressure or peak pressure, the differences are very obvious between them in cycle 3, but only peak pressure has a slight difference (3.16%) in cycle 5 as shown in fig. 6.

From aforementioned analysis, misfire generates a significant impact on the in-cylinder working process of subsequent cycles. How the misfire cycle generates effects on energy conversion and working process of subsequent cycles is analyzed in following sub-sections.

Effect on combustion process

For ICE, the in-cylinder flame propagation process directly decides the engine performances (for example, torque, fuel consumption, and emissions) [23]. The flame propagation process is mainly affected by in-cylinder mixture component and the interaction between flame propagation and flow field structure [24]. For misfire scenario, because of the existence of internal exhaust gas recirculation and lack of combustion process, it will cause obvious different for air/fuel mixture component and flow field structure in the following cycles relative to the normal scenario. Figure 7 displays the evolution of C_8H_{18} and O_2 mass fraction with CA evolved in cycle 3 (the next cycle of misfire cycle). It can be found that some of C_8H_{18} and O_2 from misfire cycle were remained in cylinder, they will take part in the combustion process of the next cycle with fresh air/fuel mixture when the intake valve opens (IVO) at cycle 3. This process will obviously impact the λ of cycle 3 (the λ of cycle 3 is 0.97 in misfire scenario). The difference of λ affect the combustion process at two aspects. First, for heat release, the reserved fuel from misfire cycle is about $6.385 \cdot 10^{-7}$ kg (before ignition, fuel in misfire scenario is $6.53 \cdot 10^{-6}$ kg, while for normal scenario is $5.89 \cdot 10^{-6}$ kg), the heat release from misfire scenario is 10.83% higher than normal scenario. Second, for combustion process, after ignition fuel is consumed more early in normal scenario, the C_8H_{18} is firstly consumed at 20 °CA bTDC (0 °CA is defined as combustion TDC), misfire scenario occurs at 10 °CA bTDC (see the black solid line in fig. 9). Then in-cylinder mixture is consumed quickly, the C_8H_{18} is consumed fastly during aTDC 7 °CA to aTDC 14 °CA for normal scenario, while this stage occurs in aTDC 11 °CA to aTDC 16 °CA for misfire condition. A similar phenomenon is also reflected in fig. 8. It shows the evolution of in-cylinder temperature and HRR with CA. It can be seen that the in-cylinder temperatures begin to rise at 1 °CA bTDC for them. For normal scenario, the fastest rise stage of in-cylinder temperature is approximatively aTDC 9 °CA to aTDC 19 °CA, and the in-cylinder temperature rises to the highest at aTDC 21 °CA, while for misfire scenario, the fastest rise stage of in-cylinder temperature occurs about aTDC 14 °CA to aTDC 24 °CA, the in-cylinder temperature reaches to highest at aTDC 29 °CA. Their differences in working process are caused by heat release process. The heat release of normal

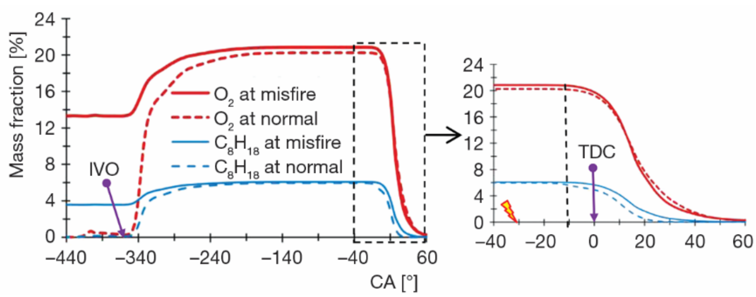

Figure 7. The comparison of C_8H_{18}, O_2 consumption between misfire and normal scenario in cycle 3

scenario is earlier than misfire scenario benefit from the earlier fuel consumption. Finally, with the C_8H_{18} is consumed fully, the in-cylinder temperature begins to decrease.

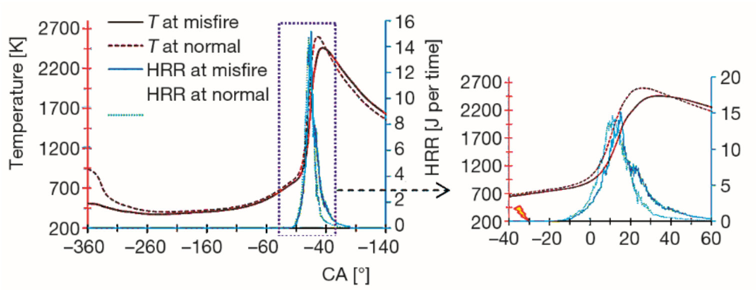

Figure 8. The evolution of in-cylinder temperature and HRR with CA in cycle 3

From aforementioned description, it can be found that although the heat released from misfire scenario is 10.8% higher than normal scenario in cycle 3, while the P_{max} of normal scenario is 13.8 % higher than misfire scenario. The difference of 24.6 % is generated by the following aspects: For misfire scenario the combustion period is longer and the cylinder wall temperature is lower because of the misfire, thus the heat transfer loss is larger. In the fast rise stage of temperature, normal scenario is closer to TDC; it means that the volume efficiency of normal scenario is higher. Relative to misfire scenario, the P_{max} or highest temperature occur earlier for normal scenario, and its combustion period continues more short, resulting in higher in-cylinder temperature, however, the aforementioned phenomena are generated strongly dependent on flame propagation, furthermore it is decided by the evolution of flow field.

According to Daniele *et al.* [25] and our previous study [5], it is well known that flame propagation is largely affected by the interaction between combustion and flow field structure. The TKE is an important parameter for flow field structure, which can directly reflect the pulsation velocity of turbulence, it is calculated by eq. (1). Figure 9 gives the evolution of TKE with CA evolved for in-cylinder average and at spark plug location, respectively. It can be seen that before exhaust valve close (EVC) in cycle 2, TKE of misfire scenario is obviously higher than normal scenario, but it also dissipates fastly. This phenomenon is generated by exhaust backflow, because cycle 2 is misfire, thus the in-cylinder pressure is very low. When the exhaust valve is opened, the environment air will enter into cylinder due to pressure difference and generate higher TKE as shown in before EVC (bEVC) 20 °CA of fig. 10 (it is displayed from A-A direction), the obvious exhaust backflow can be observed. With the decrease of pressure differential, the TKE reduces fastly. Until to EVC timing, their

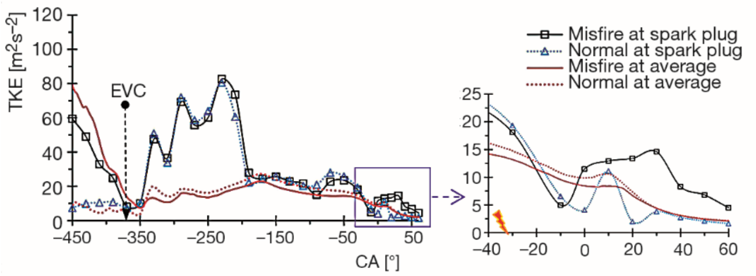

Figure 9. The evolution of TKE with CA in cycle 3

TKE are close and enter the next cycle. Although exhaust backflow has no obvious effect on flow field strength, it has a significant impact on their flow field structure. The normal scenario generates a uniform flow field and not yet produces an apparent macroscopic vortex motion, the misfire scenario generates an obvious vortex which locates in bottom right corner of chamber as EVC shown in fig. 10.

$$k = \frac{3}{2} u_i I^2 \tag{1}$$

where u_i is gas velocity and I is the turbulence intensity.

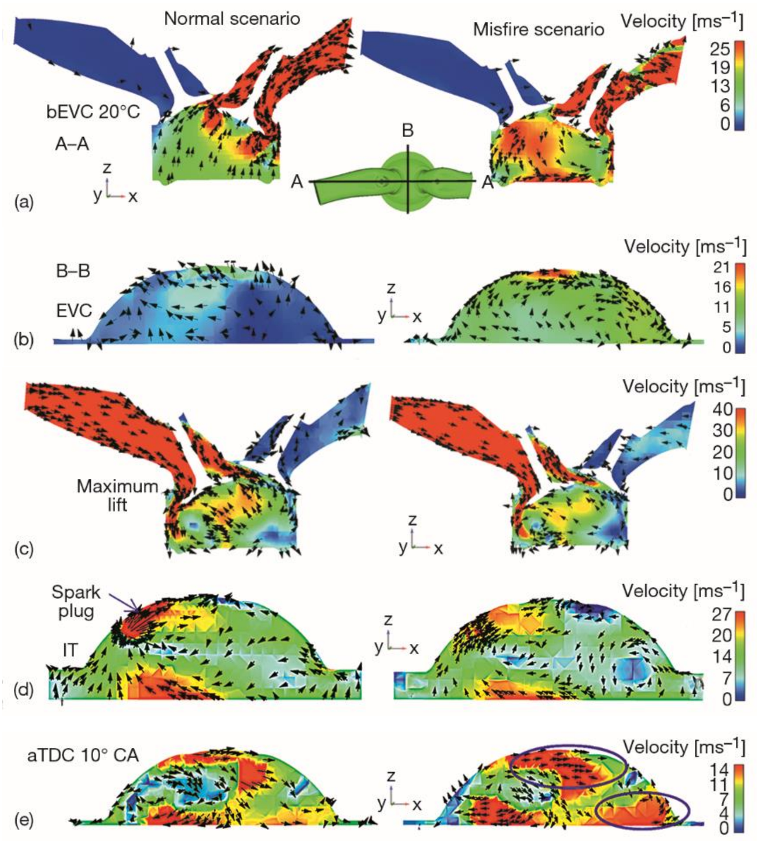

Figure 10. The comparison of flow field structure between normal and misfire scenario at different timing in cycle 3

Then the intake valve is opened, the in-cylinder average TKE has a slight rise, but TKE near spark plug has an obvious rise as shown in fig. 10. The evolution of TKE is very similar between normal and misfire scenario. But the average TKE of in-cylinder for normal scenario is higher than misfire scenario. Besides, there is only a vortex which locates near spark plug for normal scenario, while there are two vortexes which locate in cylinder center at flow field for misfire scenario, bottom right corner respectively (in fact the vortex located in bottom right corner has generated at EVC of cycle 2) as shown in fig. 10. These differences at flow field structure between two scenarios will affect the formation of flame kernel. As shown in fig. 10, the shape of flame kernel has a significant distinction. The flame kernel generated from normal scenario presents as an ellipse, the flame kernel of misfire scenario presents as an irregularly circle. Then, with the flame propagation, the decreasing TKE transfer to a slight increase. The irregular flame front shape behaves more obvious for misfire scenario, the flame front tends to propagate for the right side. The flame front develops symmetrical for normal scenario. Subsequently, the flame begins to propagate fastly. The flame front disturbs drastically in-cylinder flow field, the TKE near spark plug has an apparent change. However, the changing process between two scenarios has an obvious difference. For normal scenario, TKE changed period from rise to decrease continues for 20 °CA, while misfire scenario continues for 45 °CA. This phenomenon is caused by the difference of flow field structure. It can be found in fig. 10, there are two vortex centers located in spark plug and right corner of chamber respectively for misfire scenario because of the exhaust backflow. With the evolution of flow field, at aTDC 10 °CA the vortex located in right corner of chamber disappears and generates local strong flow regions, which cause the rise of TKE for misfire scenario. In fact, such flow field structure in misfire scenario affects not only TKE but also more for flame propagation process.

The flame propagation process is displayed in fig. 11. It can be seen that after combustion TDC, the flame propagation speed reaches to the fastest stage. Compared two scenarios, it can be found that when flame almost fills the whole combustion chamber for normal scenario, the misfire scenario only fills about three quarters of combustion chamber. The flame is obviously impeded when it propagates toward to right side of combustion chamber. This phenomenon is mainly caused by the flow field structure, it can be observed that the vortex center located in right side of combustion chamber is squeezed to break by vortex located in combustion chamber center, the broken vortex generates a strong flow field at this region and impedes the flame propagation as shown in purple ellipse of fig. 10. Thus, the flame propagation of misfire scenario is slower than normal scenario and generates subsequent chain effects.

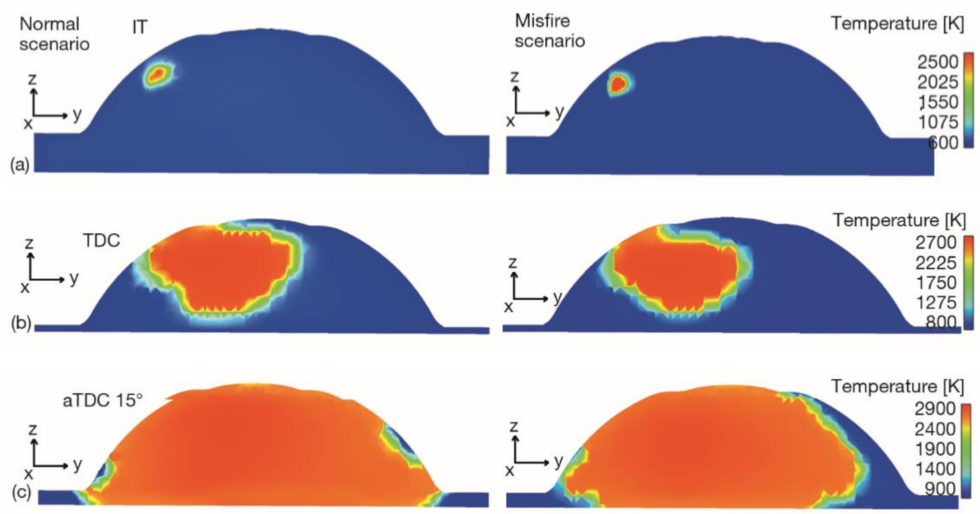

Figure 11. The process of flame propagation in cycle 3; (a) normal condition and (b) misfire condition

Effect on pollutant formation

For NO_x emissions, most of them are NO, and the proportion of NO/NO_x reaches to 90% [26]. Thus, this article also focuses on NO. According to the studies [27, 28], the generation of NO is closely related to in-cylinder temperature, oxygen concentration and residence time for reaction to take place. When λ is approximate 1 for gasoline engine the NO is mainly generated by reaction $N_2 + O = NO + N$, but dependent on in-cylinder temperature the generation speed of NO changes obviously. Bougrine *et al.* [29] found that when the in-cylinder temperature is below 2100 K, the reaction rate of NO decreased drastically. Figure 12(a) shows the NO emission for misfire and normal scenario. It can be seen that the NO generated from normal scenario is obviously higher than misfire scenario, and the generation speed of NO during combustion stage is also faster. This phenomenon is mainly caused by in-cylinder temperature and local excess air coefficient, λ. In section *Effect on combustion process*, it has known that the λ of misfire scenario is 0.97, and normal scenario is 1. The effect of λ on NO generation is very small. Thus, NO generation is dominated by in-cylinder temperature. From fig. 8, the highest in-cylinder temperature of normal scenario is 4% higher than misfire scenario, and the persistent time of high temperature (beyond 2100 K) for normal scenario is 10.36% longer than misfire scenario. This means that normal scenario will has more time and higher temperature than misfire scenario to generate NO by reaction $N_2 + O = NO + N$. Thus, normal scenario exhausts higher NO.

The CO is the intermediate production of HC fuel and toxic [30]. Our previous study [31] has described the generation and consumption pathway of CO. It is mainly generated by reaction $HCO + M = H + CO$, $HCO + O_2 = HO_2 + CO$, and it is consumed by reaction $CO + OH = CO_2 + H$. This reaction releases a lot of heat and domains the rise of in-cylinder temperature. Figure 12(b) gives CO emission for normal and misfire condition. It can be found that though the normal scenario generates more CO during combustion stage, the CO emission is close to misfire scenario, which means that more CO are consumed during main combustion phase. This phenomenon is also reflected by the evolution of CO_2 and OH, during main combustion stage the more CO_2 and OH are generated and consumed for normal scenario. This is the main reason why the higher in-cylinder temperature is acquired for normal scenario. But finally CO_2 emission is similar for them. This is because that the misfire scenario consumes more CO during post combustion stage, therefore in-cylinder temperature of misfire scenario is higher than normal scenario during post combustion stage, see fig. 8.

Figure 12(c) displays the total concentration of HC (C_8H_{18} and C_7H_{16}). It can be observed that HC is higher for misfire scenario before ignition because of misfire in last cycle. During main combustion phase, the consumption of HC for normal scenario is faster than misfire scenario. The misfire scenario of HC is higher in final emission, and normal scenario almost consumes all HC. This is because that for normal scenario the in-cylinder temperature is higher and flame propagation is faster, there are enough conditions to consume HC intermediate productions during main combustion phase. For misfire scenario, although HC are not consumed fastly during main combustion phase, the high temperature period (beyond 1500 K) continues longer than normal scenario. This phase consumes partial HC, but it is no enough to consume all HC.

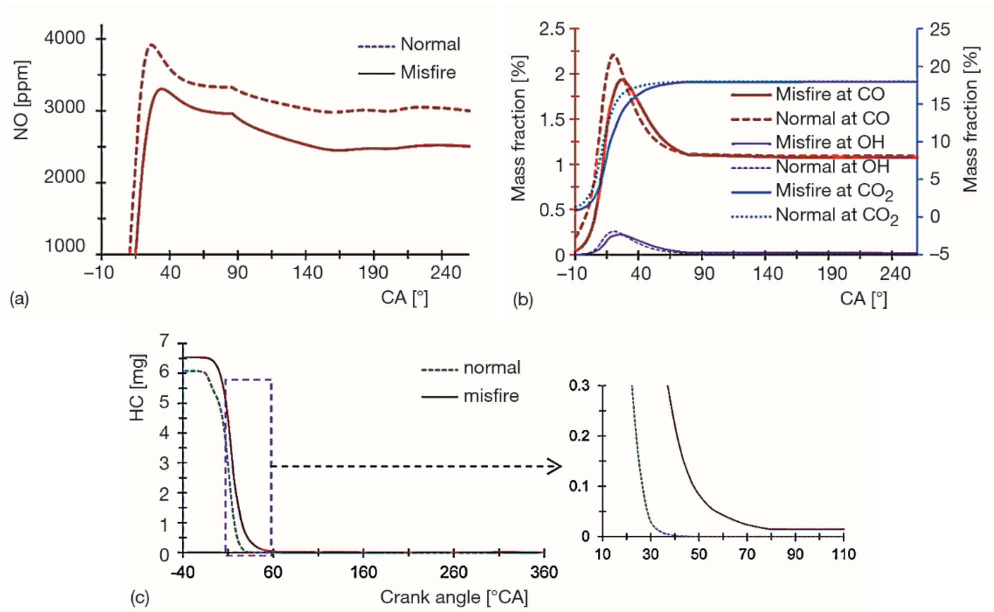

Figure 12. The comparison of emissions between misfire and normal conditions in cycle 3

Conclusions

In this paper, the effect of misfire on engine performance is discussed in detail through experiment combined with simulation. The vibration speed fluctuation rate is used to detect the misfire. In order to further understand the effect mechanism of misfire, the next cycle of misfire cycle is displayed as an example to investigate how the effect of misfire on energy conversion, combustion, and pollutant formation. Some important conclusions can be drawn as follows.

- From the wide experiment conditions, it finds that in-cylinder combustion process is more excellent under low engine speed, and the effect of load on combustion is very small. Under middle speed (5000 rpm), in-cylinder combustion process degenerates with increase of load. Under high speed (above 7000 rpm), the combination of high engine speed and low load will cause a poor combustion process. Actually, from this study, misfire is a progressive phenomenon, rather than a watershed. The effect of misfire on subsequent cycles has two respects: first, the next cycle of misfire cycle has a low in-cylinder pressure than normal condition because of the bad flame propagation and second, the effect of misfire cycle on subsequent cycles is persistent, at least its effect continues to cycle 5.
- From dissecting the interaction between flame propagation and flow field in cycle 3. The reason that misfire causes the bad working process in subsequent cycle is found. Although the heat release of misfire scenario is 10.8% higher than normal scenario, the in-cylinder pressure of normal scenario is 13.8% higher than misfire scenario in cycle 3. This is because that misfire cycle generates a vortex center due to exhaust backflow, which locates in the right side of cylinder, it fights with another vortex, which is generated by intake stage and locates in cylinder center, to cause a tanglesome flow field structure and bad flame propagation, resulting in worse in-cylinder working process.

- Comparing the emissions between two scenarios, the higher NO emission is generated for normal scenario because of the higher in-cylinder temperature. The higher HC is exhausted for misfire scenario due to the slower flame propagation, but misfire scenario has longer high temperature period (beyond 1500 K), and benefit from the longer high temperature for misfire scenario, its CO and CO_2 emissions are almost equal with normal scenario.

Acknowledgment

This research was supported by the National Nature Science Foundation of China (21776095), Guangzhou Science and Technology Project (No. 201804020048), and Guangdong key laboratory of Clean energy technology (2008A060301002). The authors appreciate the anonymous reviewers and the editor for their careful reading and many constructive comments and suggestions on improving the manuscript.

Reference

[1] ***, Ministry of Ecology and Environment of the People's Republic of China, China Mobile Source Environmental Management Annual Report, (in Chinese) 2020: http://www.mee.gov.cn/hjzl/sthjzk/ydyhjgl/201909/P020190905586230826402.pdf.
[2] Heywood, J. B., *Internal Combustion Engine Fundamentals*, McGraw-Hill., New York, USA, 1988
[3] Dhanapal, B., *et al.*, Influence of Diethyl Ether Blend in Spark Ignition Engine Performance and Emissions Operated with Gasoline and Ethanol, *Thermal Science, 20* (2016), Suppl. 4, pp. S1053-S1060
[4] Deng, B. L., *et al*., An Experimental and Numerical Investigation On Cycle-To-Cycle of Three Different Displacement Single-Cylinder Motorcycle Engines: The Sequential Analysis from Intake to Flame Propagation Process, *Fuel, 275* (2020), Sept., 117945
[5] Chen, Y. Y., *et al.,* The Influences of Ignition Modes on the Performances for a Motorcycle Single Cylinder Gasoline Engine at Lean Burn Operation: Looking Inside Interaction Between Flame Front and Turbulence, *Energy, 179* (2019), July, pp. 528-541
[6] Deng, B. L., *et al.*, The Excess Air Coefficient Effect on the Performances for a Motorcycle Twin-Spark Gasoline Engine: A Wide Condition Range Study, *Applied Thermal Engineering, 150* (2019), Mar., pp. 1028-1036
[7] Ossama, M., *et al.*, Laminar Burning Velocities at Elevated Pressures for Gasoline and Gasoline Surrogates Associated with RON, *Combustion and Flame, 163* (2015), 6, pp. 2311-2321
[8] Abhishek, S., *et al*., Misfire Detection in an IC Engine Using Vibration Signal and Decision Tree Algorithms, *Measurement, 50* (2014), Apr., pp. 370-380
[9] Jafarmadar, S., *et al.*, Numerical Studies of Spray Breakup in a Gasoline Direct Injection Engine, *Thermal Science, 15* (2011), 4, pp. 1111-1122
[10] Masayuki, T., *et al.*, Misfire Detection on Internal Combustion Engines Using Exhaust Gas Temperature with Low Sampling Rate, *Applied Thermal Engineering, 31* (2011), 17-18, pp. 4125-4131
[11] Andrew, W. O., *et al.*, Residual Generation and Statistical Pattern Recognition for Engine Misfire Diagnostics, *Mechanical Systems and Signal Processing, 20* (2006), 8, pp. 2232-2258
[12] Citron, S. J., *et al.*, Cylinder by Cylinder Engine Pressure and Pressure Torque Waveform Determination Utilizing Speed Fluctuations, SAE Transactions, SAE 890486, 1989
[13] Ren, Y., Detection of Knocking Combustion in Diesel Engines by Inverse Filtering of Structural Vibration Signals, Ph. D. thesis, The University of New South Wales, Australia, 1999
[14] Shiao, Y., *et al*., Misfire Detection and Cylinder Pressure Reconstruction for SI Engines, SAE Paper No. 940144, 1994
[15] Richards, K. J., *et al.*, CONVERGE (Version 2.1) Manual, Middleton, WI: Convergent Science, Inc.; 2013
[16] Basha, S. A., *et al.*, In-cylinder Fluid Flow, Turbulence and Spray Models, A Review, *Renewable and Sustainable Energy Reviews, 13* (2009), 6-7, pp. 1620-1627
[17] Liu, Y. D., *et al*., Development of a New Skeletal Chemical Kinetic Mode of Toluene Reference Fuel with Application to Gasoline Surrogate Fuels for Computational Fluid Dynamics Engine Simulation, *Energy & Fuels, 27* (2013), 8, pp. 4899-4909

[18] Rakopoulos, C. D., *et al*., Critical Evaluation of Current Heat Transfer Models Used in CFD In-Cylinder Engine Simulations and Establishment of a Comprehensive Wall-Function Formulation, *Applied Energy, 87* (2010), 5, pp. 1612-1630
[19] Sarli, V. D., *et al*., Large Eddy Simulation of Transient Premixed Flame-Vortex Interactions in Gas Explosions, *Chemical Engineering Science, 71* (2012), Mar., pp. 539-551
[20] Chen, J., *et al*., Improved Automated Diagnosis of Misfire in Internal Combustion Engines Based on Simulation Models, *Mechanical Systems and Signal Processing, 64* (2015), Dec., pp. 58-83
[21] Bahri, B., *et al.*, Understanding and Detecting Misfire in an HCCI Engine Fueled with Ethanol, *Applied Energy, 108* (2013), Aug., pp. 24-33
[22] Peterson, B., *et al*., High-Speed Image Analysis of Misfire in a Spray-Guided Direct Injection Engine, *Proceedings of the Combustion Institute, 33* (2011), 2, pp. 3089-3096
[23] Samet, C., *et al.*, Operating Range, Combustion, Performance and Emissions of an HCCI Engine Fueled with Naphtha, *Fuel, 283* (2021), Jan., 118828
[24] Ozgur, O. T., *et al*., Comparison of Flow Field and Combustion in Single and Double Side Ported Rotary Engine, *Fuel, 254* (2019), Oct., 115651
[25] Daniele, S., *et al*., Flame Front/Turbulence Interaction for Syngas Fuels in the Thin Reaction Zones Regime: Turbulent and Stretched Laminar Flame Speeds at Elevated Pressures and Temperatures, *J. Fluid Mech, 724* (2013), June, pp. 36-68
[26] Kwon, S., *et al*., Characteristics of On-Road NOx Emissions from Euro 6 Light-Duty Diesel Vehicles Using a Portable Emissions Measurement System, *Science of the Total Environment, 576* (2017), Jan., pp. 70-77
[27] Andrea, T. D., *et al.*, The Addition of Hydrogen to Gasoline-Fuelled SI Engine, *International Journal of Hydrogen Energy, 29* (2004), 14, pp. 1541-1552
[28] Challen, B., *et al., Diesel Engine Reference Book,* 2nd ed. England: Butterworth and Heinemann Publishing, Oxford, UK, 1999
[29] Bougrine, S., *et al*., Veynante, Simulation of CO and NO Emissions in a SI Engine Using a 0D Coherent Flame Model Coupled with a Tabulated Chemistry Approach, *Applied Energy, 113* (2014), Jan., pp. 1199-1215
[30] Feng, R. H., *et al*., Experimental Study on SI Engine Fuelled with Butanol-Gasoline Blend and H_2O Addition, *Energy Conversion and Management, 74* (2013), Oct., pp. 192-200
[31] Deng, B. L., *et al*., The Effect of Air/Fuel Ratio on the CO and NOx Emissions for a Twin-Spark Motorcycle Gasoline Engine Under Wide Range of Operating Conditions, *Energy, 169* (2019), Feb., pp. 1202-1213

Paper submitted: June 6, 2021
Paper revised: September 5, 2021
Paper accepted: September 12, 2021